Introduction

Under this contract, work was carried out on three Tasks:

I. Anode catalysts resistant to CO poisoning.

II. Cathode supports for Pt catalysts.

III. W-Ti-C catalysts.

Under Task I, studies of H_2 oxidation on Pt supported on WC were carried out. Under Task III, similar studies of $W_{1-x}Ti_xC_{1-y}$ alloys were performed. As will be seen, these efforts were in a sense, two aspects of the same problem. Useful insight into the mechanism of catalysis on transition metal carbides has been obtained, with obvious implications for the preparation of improved non-noble metal catalysts.

Task II was to have been directed at exploring the utility of TaN and TaB as Pt cathode supports. Our early work in this series showed them to have exceptional stability in acid at cathodic potentials. Due to limitations in funding and promising early results under Task I and II, this work was barely begun. One dispersion of Pt on TaN was prepared, but the catalyst was neither characterized or tested. The rest of this report deals only with Task I and II.

Task I. Anode catalysts resistant to CO poisoning.

(A) Summary and Conclusions

Work under this task was motivated by the possibility that by supporting highly active Pt on moderately active, CO tolerant WC, an anode catalyst with intermediate activity and CO tolerance might be achieved. This possibility was suggested by observation by Bockris and McHardy [1] of enhanced specific activity of cathodic reduction of O_2 supported on sodium tungsten bronze, and by the likelihood [Hamilton, 2] that Pt will segregate to the WC surface, perhaps forming monolayer or sub-monolayer coverage.

We present evidence here that Pt can be very finely (perhaps monatomically) dispersed on WC. CO tolerance far superior to that of Pt is indicated, with exchange current density four times that of the supporting WC in CO free-dilute H_3PO_4, H_2-oxidation transfer coefficient of .5 (vs ≃ .3 for WC), and activity loss of .25 in 2.7% CO/H_2 saturated dilute H_3PO_4 at room temperature. This interpretation of the data is not definitive because: (a) the basis of comparison was Pt sheet, not highly dispersed Pt; (b) the Pt/WC electrode obviously contained both a very finely dispersed and a more coarsely distributed fraction of Pt, with the result that the overall reduction in activity due to CO poisoning could only be determined by non-linear least squares fitting of (probable) reaction mechanisms to the polarization curves.

(B) The Measurements

Four dispersions of Pt on WC were studied by triangular wave voltammetry and charge stripping and plating in N_2 saturated H_3PO_4. In addition, slow triangular wave voltammetry in H_2 saturated H_3PO_4 was used to determine the H_2 oxidation activity of these dispersions. One of the dispersions was tested in 2.7% CO/H_2 saturated acid. All measurements were made in 1M H_3PO_4 at 23°C, with the dispersions in the form of flooded, teflon bonded (4% teflon by weight) thin porous electrodes. As a basis of comparision, parallel measurements were carried out on Pt sheet. The slow triangular wave measurements (sweep rate typically 1.5 mVolts/sec) were compared to point by point measurements and found to yield the same polarization currents.

On the basis of these measurements, we conclude that at least a significant fraction of the Pt in these electrodes is present in a form other than a microcrystalline dispersion, possibly in a Pt-WC surface phase. The observed H_2 oxidation currents are lower than those anticipated for microcrystalline Pt dispersions, of similar surface charge, but much greater than that attainable from the host WC alone. In addition, one electrode studied in CO/H_2 saturated acid shows H_2 oxidation current significantly higher than that available from the host WC, while the reduction in activity due to the presence of CO is an order of magnitude less than that observed

on Pt sheet.

Pt was dispersed on WC by precipitating chloroplatinic acid from aqueous solution, drying at 60°C in flowing N_2 overnight, and reducing for 4 hours at 400°C in flowing H_2. The WC used was well characterized, of low exchange current density, specific charge and BET area. These parameters and the two Pt loadings used are listed in Table 1. The porous electrodes were prepared in a manner similar to that of Vogel and Lundquist [3] by mixing 4 w/o PTFE-30 with the powders, and spreading an aqueous slurry of this mixture on teflon tape supported on Ta sheet. After air drying, this assembly was sandwiched between Al foils and hot pressed at 310°C under 10,000 Newtons total force. Al was dissolved in 20% NaOH and the electrode thoroughly washed, neutralized in dilute H_3PO_4, air dried, and lifted from the Ta support. The electrode was pressed at its edge against a Ta electrical contact (we have found Ta to be passive in the overpotential range of our measurements in H_3PO_4 [4]) by a teflon screw. The free electrode surface was exposed to gas saturated (H_2, CO/H_2, N_2) acid. Measurements were made with the electrode flooded in an all-teflon cell using a Pt counter electrode and a dynamic Pt reference electrode.

In Table 2 are listed various parameters characterizing the 4 dispersions studied. Column 1 gives the Pt loading; column 2 the surface charge, Q_S, obtained by averaging the results of

anodic and cathodic charging curves carried out between 0.02 and 0.30 volts (RHE). Columns 3 and 4 give the mass of Pt, m_{Pt}, and total WC BET area, A_{WC}, of each electrode. Column 5 lists the parameter

$$f = \frac{\text{number of surface Pt atoms}}{\text{total number of Pt atoms}},$$

the estimated surface fraction of Pt obtained by assuming that the measured surface charged is due solely to hydrogen ions which occupy surface Pt atoms on a one to one basis.

Column 6 lists the Pt specific surface area

$$A_{Pt} = \frac{Q_s - Q_s^{WC}}{190 \times M_{Pt}}$$

obtained by using 190×10^{-6} C/cm^2 as the metric, and taking

$$Q_s^{WC} = 0.8 \times 10^{-6} x A_{WC}$$

as an upper limit to the charge associated with uncovered WC. ($Q_s^{WC} << Q_s$

In column 7, the parameter

$$a = \frac{Q}{A_{WC}}$$

is listed. As will be evident later, of all these parameters, a correlates best with performances of these electrodes.

The loading for dispersion 3 is marked with a star. The surface of electrode 3 was accidently reconstructed from electrode 1 by operation at corrosive overpotential (>0.4 Volts RHE). This reconstruction took place during slow triangular wave measurements in H_2 saturated acid, before charging curve measurements were carried out. Hence, for electrode 1, Q_s, f, A_{pt}, and a, which are bracketed in Table 2, are estimated from the measured H_2 oxidation current at 0.3 volts (RHE), on the basis of observed linear variation of Q_s with activity at 0.3 volts for electrodes 2, 3, and 4. This surface reconstruction will be considered in more detail later.

In Fig. 1 triangular wave sweeps made on Pt sheet and electrode 4 (A_{Pt} = 34 m^2/gm) are compared. The peaks at 0.03 volts for Pt sheet and at 0.07 volts for electrode 4 are H_2 oxidation maxima. The behavior of electrode 4 is typical of each of the Pt/WC electrodes studied; no hydrogen adsorption extrema are observed. Blurton et al. [5] have reported observation of these extrema on carbon supported microcrystalline Pt dispersions with Pt specific areas as high

as $50 m^2/gm$. Yet they are absent on all 4 Pt/WC dispersions, even at calculated specific areas as low as 37 and 34 m^2/gm. This suggests that conventional assessment of Pt specific surface area is probably meaningless for these Pt/WC catalysts, and that some significant fraction of the Pt in these electrodes is very highly dispersed.

In Fig 2, we address the question of the H_2 oxidation performance to be expected if our Pt dispersions were distributed as microcrystals of the specific surface areas indicated in Table 2. In this event, we expect polarization curves in H_2 to follow the form predicted and observed by Vogel et al. [6]. In fig 2, the extremes of behavior expected for current normalized to the limiting current for mixed activation and diffusion (upper curve) and for pure activation (lower curve) control are displayed. When so normalized, the limiting shapes depend only on the equilibrium value of hydrogen coverage, θ_0. The value $\theta_0 = 0.7$, which we obtained for Pt sheet in 1M H_3PO_4 at 23°C (see below), was used in this plot. If, for our electrodes, the calculated specific areas and other appropriate parameters are inserted in the general (not the limiting) expression, mixed control behavior is obtained. The activity of the WC support is so low that in pure H_2, it may be neglected. We will show this presently.

In fact, the hydrogen polarization curves obtained with our electrodes show distinctly different behavior. Fig. 3 shows the observed currents normalized at 0.3 volts. Like the thick porous electrode curve repeated here in dashes, these electrodes all show high current at low overpotential, but they do not limit out. Moreover, the greater the ratio of measured specific charge to WC area, the greater the discrepancy between the observed and expected polarization curves. This behavior again strongly suggests that two different types of Pt are present in these electrodes: a normal component, and one which does not behave normally, which on the evidence of the linear sweep voltammagrams, is most likely in very highly dispersed form.

It is also worth noting that these Pt/WC electrodes are not affected by the presence of oxidizable impurities in the electrolyte. We anticipated problems from this source because WC must not be raised to potentials higher than .35 volts if irreversible corrosion is to be avoided. Hence the normal procedure of Pt clean up at an overpotential of about 1.0 volt is excluded. Our electrolyte is prepared by diluting once refluxed concentrated acid in triply distilled water. A freshly cleaned Pt sheet electrode poisons (as measured by both disappearance of hydrogen adsoption extrema and decay of hydrogen oxidation current) at a rate of about 0.7% per

minute. The WC supported electrodes are not visibly poisoned for periods of from 2 to 13 days in the cell. Electrolyte cleanup by dispersions in excess of those measured can be excluded. We have done Pt sheet measurements before and after porous electrode tests in the same electrolyte sample. Pt sheet poisons at the same rate before and after the porous electrode runs.

Incomplete flooding of the porous electrode is unlikely. Our electrodes absorb measurable volumes of electrolyte in good agreement with the total porosity calculated from the discrepancy between their overall density and the density of tungsten carbide. Extraodinary diffusion coefficients of the oxidizable impurities seem most unlikely. Rather, this resistance seems to be an inherent property of the catalysts, and this once again suggests that they are not typical microcrystalline platium dispersions.

A test of the CO tolerance of Pt/WC dispersions was carried out on electrode 2 in 1M H_3PO_4 at 23°C. A feed of 2.9% CO/H_2 was used. The results are shown in Fig. 4. The upper curve in solid circles is the pure hydrogen response. Crosses show the current measured in the presence of CO. The open circles show the response which would be obtained from the electrode if the WC alone were present. The difference between

pure and CO contaminated hydrogen curves for WC would lie within the circle size. The current from the poisoned electrode significantly exceeds the maximum possible current obtainable from the WC alone, due principally to a higher transfer coefficient, .5 vs .3 for WC alone.

In Table 3, the performance of electrode 2 in carbon monoxide is compared with the performance of pure Pt. The figure of merit is the ratio of currents obtained at 0.15 volts in CO/H_2 and in pure H_2. For electrode 2, the ratio of the observed currents at 0.15 volts is 100.0×10^{-3}; if the maximum possible WC current is subtracted from the observed currents, the ratio drops to 35×10^{-3}.

As a reference for Pt in dilute acid at room temperature, the current ratio on Pt sheet was obtained two ways. Simply normalizing to the observed diffusion limited current yields an upper limit of 25×10^{-3}. A more meaningful estimate is gotten by correcting the observed pure hydrogen current for the diffusion concentration gradient extending out into the acid. Fitting the observed Pt sheet curve to the current/overpotential relation for a planar platinum electrode of Vogel et al. [6] with a linear correction for the hydrogen concentration gradient yields a carbon monoxide/hydrogen current ratio of 0.8×10^{-3} at 0.15 Volts (and an equilibrium

hydrogen coverage in CO free acid of θ_o = 0.7 as well). Some additional indication can be obtained by extrapolating data obtained by Vogel et al. [6] and Stonehart and Ross [7] with 1.7% carbon monoxide in hydrogen on porous electrodes in mixed control, at high temperatures and in concentrated acid, to room temperature. Here a current ratio of 0.1×10^{-3} is obtained.

An interesting point is the reconstruction of dispersion 1 into dispersion 3 alluded to above. The time course of this event is shown in Fig. 5. The sample was swept between 0.0 and 0.58 volts (well into the region of irreversible oxidation of WC) at a rate of 2.3 mVolts/sec. On the fourth sweep, in H_2 saturated acid, the current suddenly dropped, and remained stable at the new level for 3 additional sweeps. (Voltage was maintained, and the pen lifted until the voltage reached zero.) Thereafter, the maximum voltage applied to this and other dispersions was kept at 0.33 volts or less.

The data described above for Pt dispersed on WC suggest that Pt is present in two forms: as microcrystalline Pt and a surface dispersion of Pt-W-C. Some uncovered WC may also be present. Various unsuccessful attempts to produce Pt/WC dispersions free of microcrystalline Pt, and thus permit direct determination of the properties of the hypothesized surface Pt-W-C dispersion, were unsuccessful. We therefore attempted

to assess the validity of the simple three catalyst picture by computer modelling of the available data. Polarization data in 2.9 CO/H_2 saturated acid suggest that the Pt-W-C catalyst follows simple Tafel kinetics with transfer coefficient α= 0.5. WC shows Tafel kinetics with $\alpha = 0.3$ [8]. The kinetic relation for Pt has been derived by Vogel et al. [6]. The loss in activity for Pt in the presence of CO is attributed to simple site blockage [6]. Assuming the same to hold true for the Pt-W-C surface dispersion, and further assuming that all three catalyst are uniformly distributed through the thin porous electrodes, it is readily shown that the H_2 oxidation current is

$$I(V) = (2FQADc_0x)\ \mathrm{TANH}(Lx)$$

where

$$x = (W_1E^2F + W_2G + W_3H)^{1/2}$$

$$E = [\Theta_0 + (1-\Theta_0)\ \mathrm{EXP}(FV/RT)]^{-1}$$

$$F = \mathrm{EXP}(2FV/RT)$$

$$G = \mathrm{EXP}\ (\alpha_2 FV/RT)$$

$$H = \mathrm{EXP}\ (\alpha_3 FV/RT)$$

$W_i = (f_i\ \gamma_i\ i_0^i)/2FDc_0$ with i = 1 for Pt, 2 for WC, and 3 for Pt-W-C.

Here I is electrode H_2 oxidation current,

V - overpotential, F the Faraday constant, Q - electrode roughness factor,

A - electrode cross section area, L - electrode thickness,

D - the H_2 diffusion coefficient, c_0 - the H_2 saturation

concentration, θ_0 - the equilibrium hydrogen coverage on Pt, R the gas constant, T - the absolute temperature, α the transfer coefficient, i_0 exchange current density, γ - catalyst surface areal density and $0 \leq f \leq 1$ the catalyst poisoning factor.

We have also assumed the hydrogen reaction equilibrium potential to be the same on all catalysts, and proton diffusion to be much faster than H_2 molecule diffusion.

Starting values of θ_0, f, and i_0 for Pt in 1M H_3PO_4 at 23°C have been obtained by fitting H_2 oxidation data on Pt sheet. For WC, α, i_0, and f = 1 are known. For Pt-W-C, α, and i_0 are deduced from polarization curves obtained with 3% CO/H_2 and f is a disposable parameter.

The fitting procedure is non-trivial, for the fitting function is ill behaved. Best results were obtained by assuming that all WC-active sites were occupied by Pt, and varying the crystalline Pt to Pt/WC area ratio along f_2 cuts. Results are displayed in Fig. 6 as a reconstruction, circles, of the polarization curve in pure H_2 - saturated acid from the fitted parameters. The measured curve is the open loop, with height indicating the reproducibility of the polarization measurements in H_2, and width reflecting the uncertainty in reference potential resulting from the use of a

dynamic hydrogen reference electrode. In summary, the Pt/WC dispersion appears to obey Tafel kinetics with a transfer cofficient of 0.5, with an exchange current density four times that of the host WC. Operation in 2.9%CO/H_2 feed, in 1M H_3PO_4 at room temperature reduces the H_2 oxidation exchange current density by a factor of 0.25.

TASK III W-Ti Carbide Catalysts

(A) Summary and Conclusions

H_2 evolution and oxidation were studied on the bcc structure alloy system $W_{1-x}Ti_xC_{1-y}$ over the composition ranges $0 \leq 1-x \leq .47$, $.03 \leq y \leq .09$, in 1M H_3PO_4 at room temperature and in 85 wt% H_3PO_4 at 54 and 70°C. Measurements were made on flooded, porous, teflon bonded, thin electrodes, prepared by the method described under Task I, in the same apparatus. Relevant results are: (1) complete tolerance of CO in the H_2 feed; (2) simple Tafel kinetics, with transfer coefficients suggesting proton discharge as rate limiting; (3) exchange current densities varying approximately as $y(1-x)^2$, suggesting an active site consisting of a surface carbon defect with at least two tungsten near neighbors; activation energy of (7 ± 2)kcal/mol.

The more active catalyst, WC_{1-y}, displays similar reaction kinetics and activation energy (see [8] and references therein), and, as we point out here, a similar dependence on the carbon defect y. If the activities of WC_{1-y} and $W_{1-x}Ti_xC$ are adjusted to the same temperature, acid concentration, surface atom density, and probability of near neighbor W atoms (by dividing the $W_{1-x}Ti_xC_{1-y}$ activity by $(1-x)^2$), and plotted against y, they group along a line with zero intercept and positive slope. Thus both catalysts would

appear to have the same type of active site. The $W_{1-x}Ti_xC_{1-y}$ is active naturally, since equilibrium alloys of this system exist over a wide range of y values [9]; the highly active samples of WC_{1-y} are active in view of their metastable carbon defect concentrations,the range of y in equilibrium WC being nil. [10].

We stress that these conclusions are by no means definite. The experimental numbers support them, but probable errors in the data are large. Particularly troublesome uncertainties arise from the difficulty of estimating carbon defect densities in WC_{1-y} and experimental problems in the $W_{1-x}Ti_xC_{1-y}$ measurements, due to incomplete wetting of these electrodes at higher W concentrations. The underlying assumption of equal bulk and surface W and carbon defect concentrations in $W_{1-x}Ti_xW_{1-y}$ is also open to question.

The results of the $W_{1-x}Ti_xC_{1-y}$ studies are summarized in Table 4. Typical polarization curves are shown in Fig. 7.

The functional dependence of i_o on y and 1-x was tested by comparing i_o, y, (1-x), $(1-x)^2$, y(1-x), and $y(1-x)^2$, all normalized for convenience at the (1-x = .23, y = .03) point. Values of

$$\chi^2 = \Sigma_i \frac{(i_o - f_i)^2}{f_i}$$

f_i being the appropriate function of y and (1-x) at the i^{th} data point, were 45.8, 68.6, 19.7, 11.2, and 0.8 in the fitting function order listed above.

(B) The measurements

Measurements of H_2-oxidation on $W_{1-x}Ti_xC_{1-y}$ present several practical difficulties. Effective surface capacitance is large; low frequency triangular wave voltammetry can produce quite erroneous results, and point by point measurement of the polarization curves must be carried out. The exchange current density is low, and there is a large polarization current in inert gas saturated acid. To determine the H_2 oxidation current, measurements must be very carefully made in both H_2 and N_2 saturated acid. Also, at higher W-content, the alloy is a poor wetter.

W-free TiC has been reported to be inactive.[11,12]. We could detect no activity in TiC either.

Electrodes were prepared by the method described under Task I, and measurements were carried out with the same cell and apparatus.

Cubic structure of the samples was verified by X-ray diffraction. The samples were supplied in powder form by Kennametal, Inc., together with their chemical analysis. BET area measurements were carried out by the Micromeritics Instrument Corp.

All of the samples were cursorily checked for CO tolerance in 1M H_3PO_4 at 23°C, and appeared not to be poisoned. The 1-x = .47 sample was more carefully checked. In the overpotential range $0.03 \leq V \leq .16$ volts (RHE), $\Delta V = .01$ volts, with 2.9%CO/H_2 and H_2 feeds, the mean fractional difference in H_2 oxidation current between the CO contaminated and pure feed curves was -2.5%. This lies Within the reproducibility of the measurements, but strongly indicates that in these compounds, as in WC and $Mo_{1-x}W_xC$, CO is neither oxidized nor acts as a poison, but rather, simply dilutes the H_2 feed. These data were obtained on an incompletely wetted sample. But at no time was there any increase in activity which would be expected from increased wetted area.

Polarization studies at 54 and 70°C in 85 w/o H_3PO_4 were carried out on the 1-x = .44 sample which also was incompletely wetted. Two problems arose here. Progressive wetting can not be completely ruled out. We went from low temperature to high, and did not recheck at low temperature. However, no change was observed during any of the repetitive runs. In addition to this uncertainty, a progressive shift in the polarization curves with temperature was observed. Checking the apparatus via voltammetric sweeps on a Pt sheet electrode, using for reference the mean positions of the two strong H adsorption-desorption extrema, we observed temperature

dependent shifts attributable to variation in the potential of the dynamic reference electrode. These shifts can be completely eliminated with appropriate changes in the reference electrode current. Moreover, the magnitude of the shifts in the high temperature carbide data can be estimated.

Appropriate values of temperature dependent shifts in reference potential were then applied to the high temperature 1-x = .44 data, and a rough estimate made of the activation energy. For the 1-x = .44 sample, at 0.04 volts, in the activation controlled region, $E_a = 7 \pm 2$ kcal/mol, and at 0.24 volts in the mixed control region, $E_a = 3 \pm 1$ kcal/mol.

We attempted to find alternate electrolytes to overcome the wetting problem at higher W-concentrations, but were unsuccessful. The principal experimental sign of incomplete wetting was the presence of a diffusion limited region in the polarization curves of the 1-x = .44 and .47 samples. For the overall polarization currents obtained and the Tafel shape of the curves, a diffusion limited region could be anticipated only if the electrodes were incompletely wetted. No diffusion limited region was observed for the 1-x = .23 and .31 samples, for which water uptake was in good agreement with the total porosity calculated from electrode dimensions and bulk densities.

Given the current-voltage relation of thin porous electrode model with Tafel kinetics [13]

$$I(V) = QA(2FDC_0 i_o \gamma \exp[FV/RT])^{1/2} \times \tanh\left(L[i_o\gamma/2FDC_0]^{1/2} \exp[\alpha FV/2RT]\right)$$

where symbols are defined under TASK I, and the limiting cases

$$I(V) = QA(2FDC_0 i_o \gamma)^{1/2} \exp[\alpha FV/2RT] \text{ for } V \to \infty$$

$$I(V) = QAL\gamma i_o \exp[-\alpha FV/RT] \text{ for } V \to 0, \text{ and the relation}$$

$$L(i_o\gamma/2FDC_0)^{1/2} = \exp[-\alpha FV_c/2RT]$$

which holds at the potential V_c of the intersection of the high and low V limiting cases, true L and γ can be inferred for the incompletely wetted electrode. Propagation of uncertainties in this procedure leads to the high uncertainties quoted for i_o at $1-x = .44$ and $.47$

It becomes interesting then, to compare the activity of WC_{1-y} with that of $W_{1-x}Ti_xC_{1-y}$. This is done, on the basis of presently available data, in Fig. 8. Note that we are now focusing attention on the effect of carbon deficiency in WC_{1-y}. The WC_{1-y} data displayed were taken from the work of Ross and Stonehart [14] who provided not only measured activities on a number of differently prepared samples, but total carbon content and Auger analyses of these samples as well. From the compositional data, two estimates of the carbon deficiency can be made, assuming the W-sublattice to be full (behavior characteristic of the transition metal

monocarbides). The horizontal width of the WC_{1-y} blocks in Fig. 8 reflects the difference in these estimates. The measured activities at 0.05V were adjusted to 54°C using E_a = 9000 cal/mol, the value we obtained for near zero overpotential [8]. An uncertainty of 10% was assumed for the measured currents.

For the $Ti_{1-x}W_xC_{1-y}$ alloys, some adjustment must be made for the non-unity W exchange. If the assumed reaction mechanism is valid and no strong surface segregation occurs, the activity of these alloys is expected to vary at least as $(1-x)^2$, the probability of two W atoms occurring as surface near neighbors, as noted above. The spread of y values for the Ti alloys in Fig. 8 were obtained from chemical analyses, and from reported values [9] of the δ + C two phase boundary at 1500°C. (All but one sample showed unreacted carbon.) Only one sample, x = .31, shows notable deviation from the phase diagram data. Uncertainties in i_o for $W_{1-x}Ti_xC_{1-y}$ result from those of fitting the characteristic curves, BET area, and electrode geometry, and in the cases of 1-x = .44 and .47, from the propagation of these uncertainties in estimating effective values of the geometrical constants of the electrodes. Adjustments to 54°C in concentrated acid were made by scaling data for all 4 samples by the factor observed for the 1-x = .44 sample. Also, a factor accounting for the

different surface cell densities of the alloys was used.

Despite the large uncertainties in the data displayed in Fig. 8, a definite dependence on bulk carbon deficiency is indicated, with no distinction discernible between the activity dependence of the cubic and hexagonal carbides on bulk carbon deficiency. Taken together these data suggest that the active sites on W-C H_2 oxidation catalysts consist of 2 or more W near neighbors of a C surface defect.

References

1. Bockris, J.O.M. and McHardy, J., J. Electrochem. Soc. 120, 61 (1973).

2. Hamilton, J.C., Phys. Rev. Letters 42, 9189 (1979).

3. Vogel, W.M., and Lundquist, J.T., J. Electrochem. Soc., 117, 1512, (1970).

4. Bennett, L.H., Cohen, M.I., Dragoo, A.L., Franklin, A.D., McAlister, A.J., and Young, K.F., Materials for Fuel Cells, NBSIR 77-1270, 1977. (National Technical Information Service, Springfield, VA 222151).

5. Blurton, K.F., Greenberg, P., Oswin, H.G., and Rutt, D.R., J. Electrochem. Soc., 119, 559, (1972).

6. Vogel, W.M., Lundquist, J.T., Ross, P.N., and Stonehart, P., Electrochimica Acta, 20, 79, (1975).

7. Stonehart, P., and Ross, P.N., Electrochimica Acta, 21, 441, (1976).

8. McAlister, A.J., and Cohen, M.I., Electrochimica Acta, 25, 1685, (1980).

9. Rudy, E., J. Less Common Metals, 33, 245, (1973).

10. Hasen, M., Constitution of Binary Alloys, 2nd Ed., (McGraw-Hill New York, 1958) and references therein.

11. Bethin, J.R., Ph.D. Thesis, University of Illinois, Urbana, IL, USA, 1979.

12. Mund, K., Richter, G., and vonSturm, F., Coll. Czech. Chem. Comm., 36, 439, (1971).

13. Vogel, W.M., Lundquist, J.T., and Bradford, A., Electrochimica Acta, 17, 1735, (1972).

14. Ross, P.N., and Stonehart, P., J. Catalyst, 48, 42 (1977).

TABLE 1

PROPERTIES OF WC USED

$i_0 = 0.6 \times 10^{-7}$ A/cm^2
$Q_s = 0.8 \times 10^{-6}$ C/cm^2
} 23°C, 1M H_3PO_4

BET AREA = 0.38 m^2/gm

Pt LOADINGS

a) 0.10×10^{-6} gm/cm^2 WC AREA

b) 0.05

TABLE 2

ELECTRODE PARAMETERS

	LOADING 10^{-6}gm/cm^{2}WC	Q_s 10^{-6}Coulcmb	m_{Pt} 10^{-6}gm	A_{WC} cm^2	f	A_{Pt} m^2/gm	q 10^{-6} Coul./cm^2
1	0.10	2100	9	82	0.44	119	24.8
2	0.10	800	4	39	0.39	103	21.0
3	*	700	9	82	0.15	37	8.4
4	0.05	450	4	79	0.19	34	5.7

$$f = \frac{\text{number of surface Pt atoms}}{\text{total number of Pt atoms}}$$

$$A_{Pt} = \frac{Q_s - Q_s^{WC}}{190 \times m_{Pt}}$$

$$q = \frac{Q_s}{A_{WC}}$$

* Electrode surface reconstructed from (1) at WC-corrosive overpotential.

TABLE 3

FRACTIONAL REDUCTION OF H_2 OXIDATION ACTIVITY DUE TO POISONING

SAMPLE	ASSUMPTIONS	$i^{CO}(\eta)/i^{H2}(\eta)$
Electrode 2 Dilute acid, 23°C, 2.9%CO/H_2, pure H_2 0.15 volts	Observed i^{CO}	100.0×10^{-3}
	Observed i^{CO} less maximum WC current	35.0×10^{-3}
Pt Sheet Dilute acid, 23°C, 2.9%CO/H_2, pure H_2, 0.15 volts	i^{CO} normalized to observed diffusion limited i^{H2}	25.0×10^{-3}
	i^{CO} normalized to diffusion corrected i^{H2} (linear diffusion correction to i/η relation of Vogel et al. [6]	0.8×10^{-3}
Porous Pt electrode in mixed control Concentrated acid, 80°C ≤ T ≤160°C, 1.7%CO/H_2, 40%H_2/N_2 0.2 volts (Vogel et al.,[6]; Stonehart and Ross, [7])	Extrapolation to 23°C	0.1×10^{-3}

Table 4

Tungsten exchange, carbon defect,

and electrochemical rate constants for

$W_{1-x}Ti_xC_{1-y}$

1-x	y	i (10^{-8}A/cm^2)	α_{ox}	α_{ev}
0	---	0	---	--
.23±.01	.03±.01	.6±.2	.21±.01	.6
.31±.01	.06±.03	.8±.2	.15±.01	.4
.44±.02	.06±.01	5.0±2.5	.14±.01	.6
.47-.07	.09±.01	7.0±3.5	.28±.02	.4

Figure Legends

Figure 1. Triangular wave voltammetry at .017V/sec of Pt sheet (upper curve) and dispersion 4 (lower curve).

Figure 2. Predicted and observed behavior of porous layer electrodes of microcrystalline Pt (Vogel et al., Ref. 6) in the limiting cases: (a) mixed control; (b) activation control.

Figure 3. Observed H_2 oxidation currents on electrodes 1 (dots), 2 (crosses), 3 (diamonds), and 3 (circles). The dashed curve is the theoretical prediction for microcrystalline Pt in mixed control.

Figure 4. Effect of 2.9%CO in the H_2 feed on electrode 2. Dots: pure H_2; crosses, in 2.9%CO/H_2; circles, for the host WC alone.

Figure 5. The observed change in response of electrode 1 undergoing surface reconstruction in sites, sweep speed .0023V/sec, in H_2 saturated, 1M H_3PO_4.

Figure 6. Fitting of the pure H_2 response of electrode 2 from its CO response using crystalline Pt rate parameters obtained from Pt sheet. Circles: fitted curves; solid figure, measured response, including reproducibility of current and uncertainty in the reference potential.

Figure 7. Current density (normalized to total electrode BET area) for $W_{.24}Ti_{.76}C$ in N_2 saturated 1M H_2PO_4 at 23°C, open circles; and the H_2 oxidation current obtained as the difference between the current densities obtained in H_2 and N_2 saturated acid at positive overpotential (vs. a dynamic Pt reference electrode), filled circles.

Figure 8. Specific current density at 0.05V, 54°C, in concentrated H_3PO_4, vs y: dots, WC_{1-y}; diamonds, $Ti_{1-x}W_xC_{1-y}$. For the Ti alloy, current has been divided by $(1-x)^2$. Other adjustments to data discussed in text.

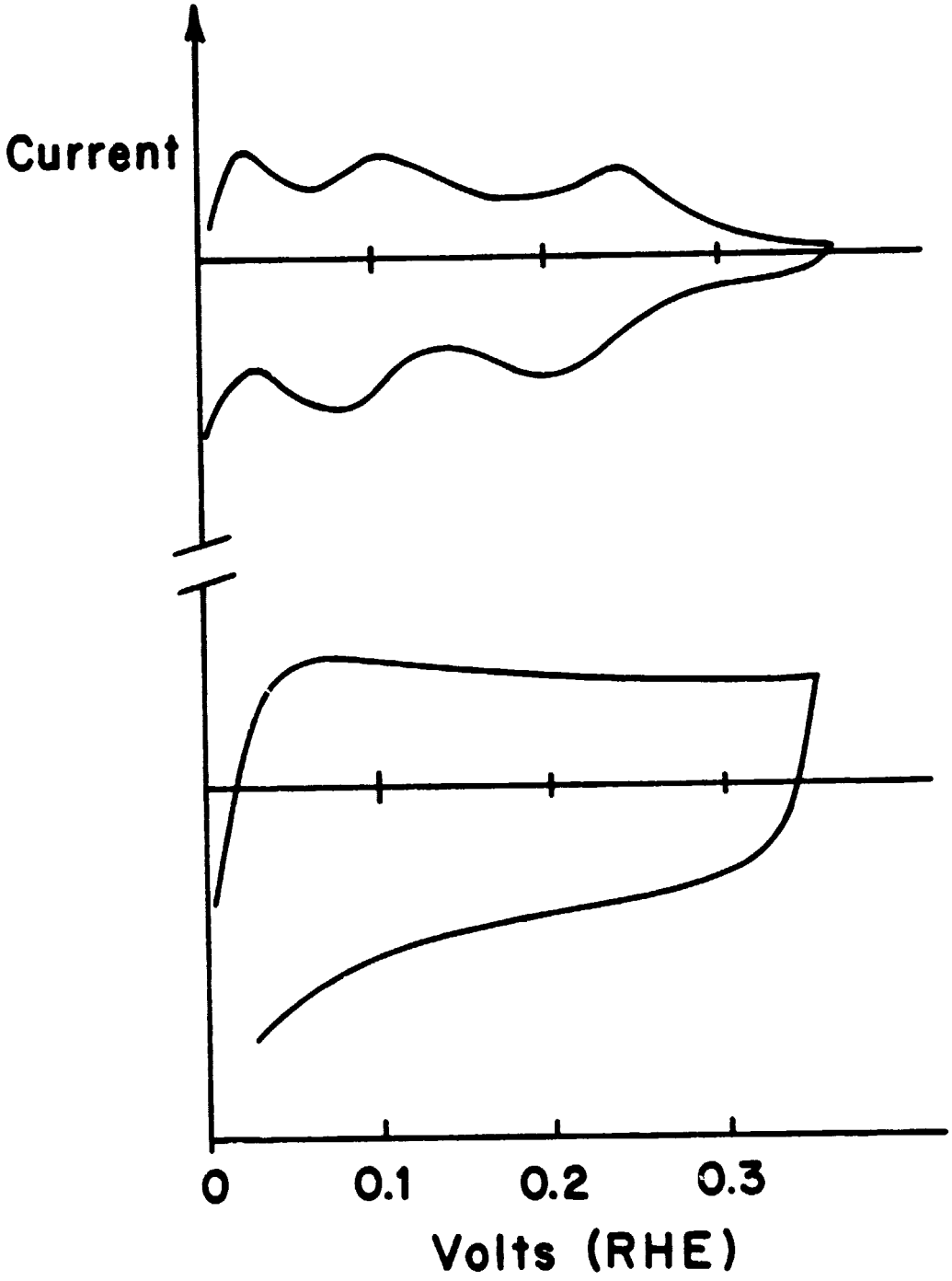

Figure 1

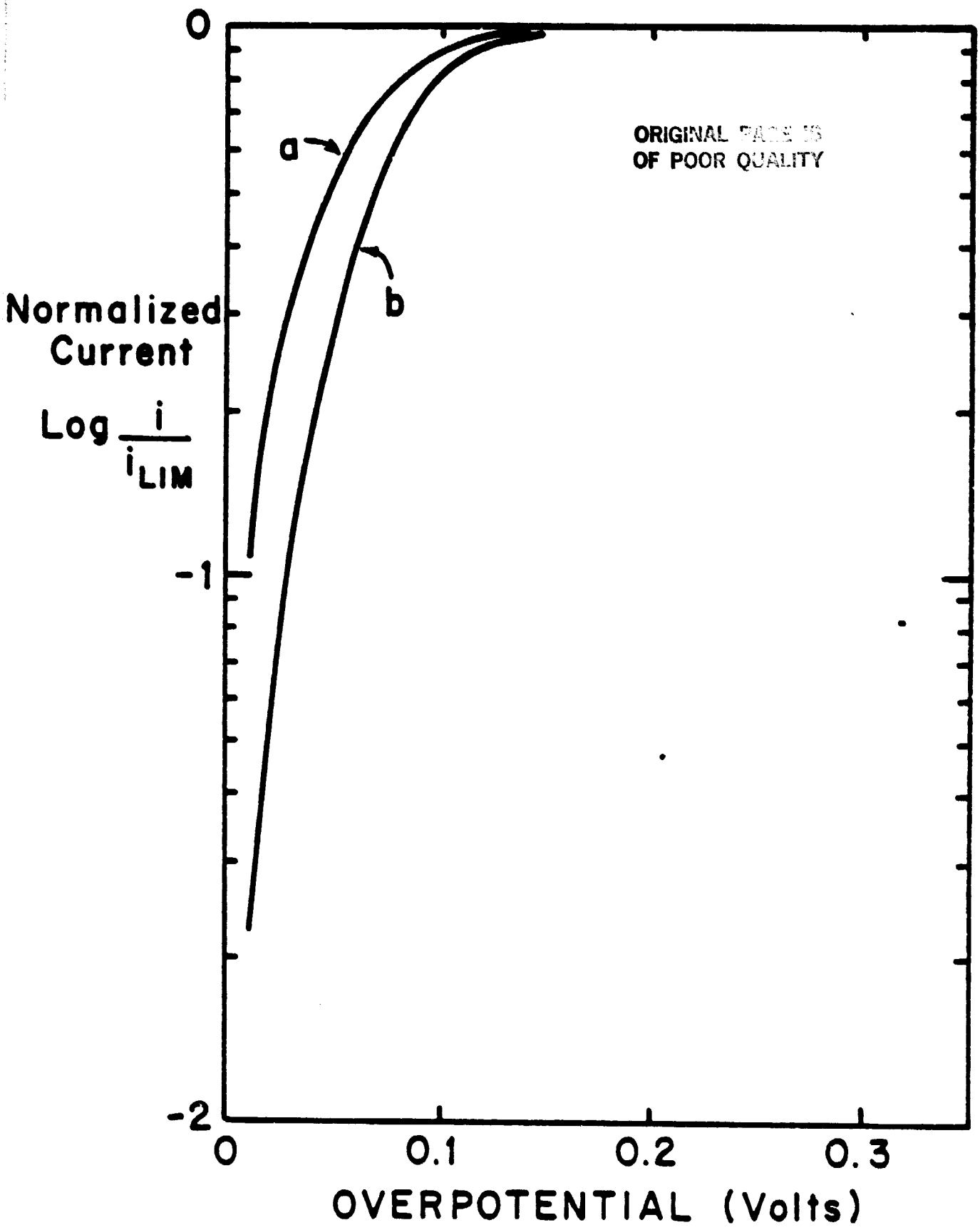

Figure 2

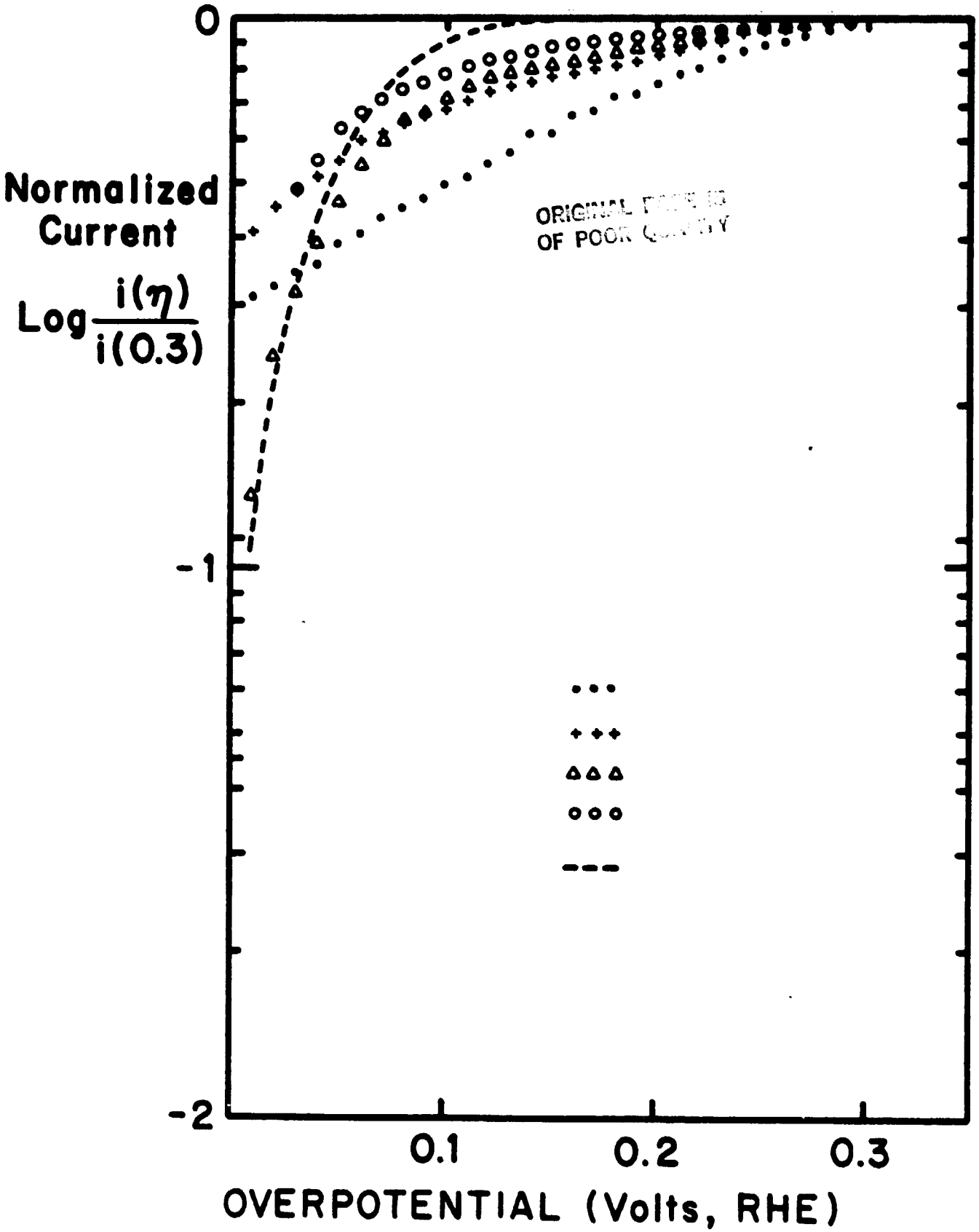
0
-1
-2
Normalized Current
Log i(η) / i(0.3)
0.1
0.2
0.3
OVERPOTENTIAL (Volts, RHE)

Figure 3

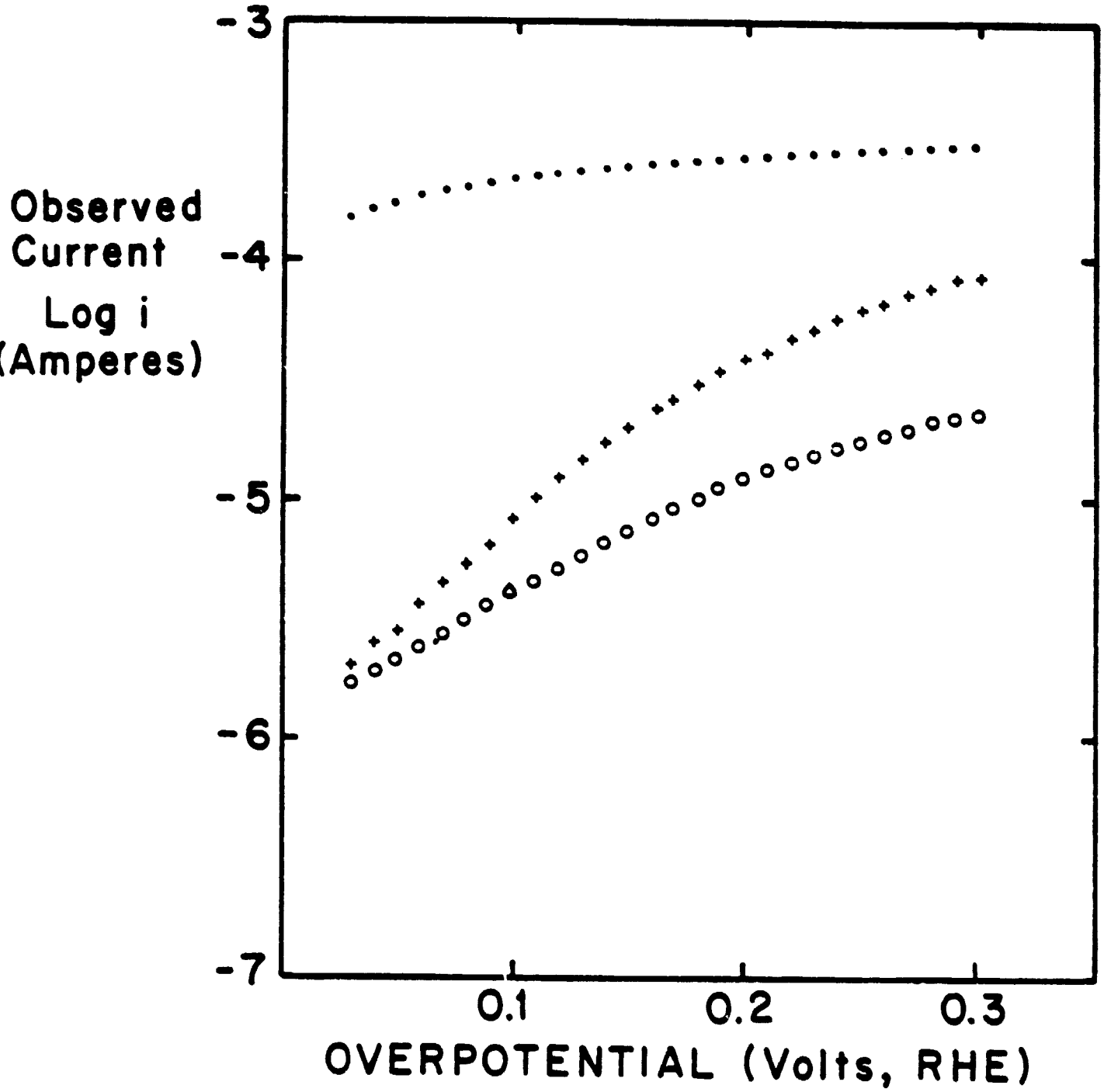

Figure 4

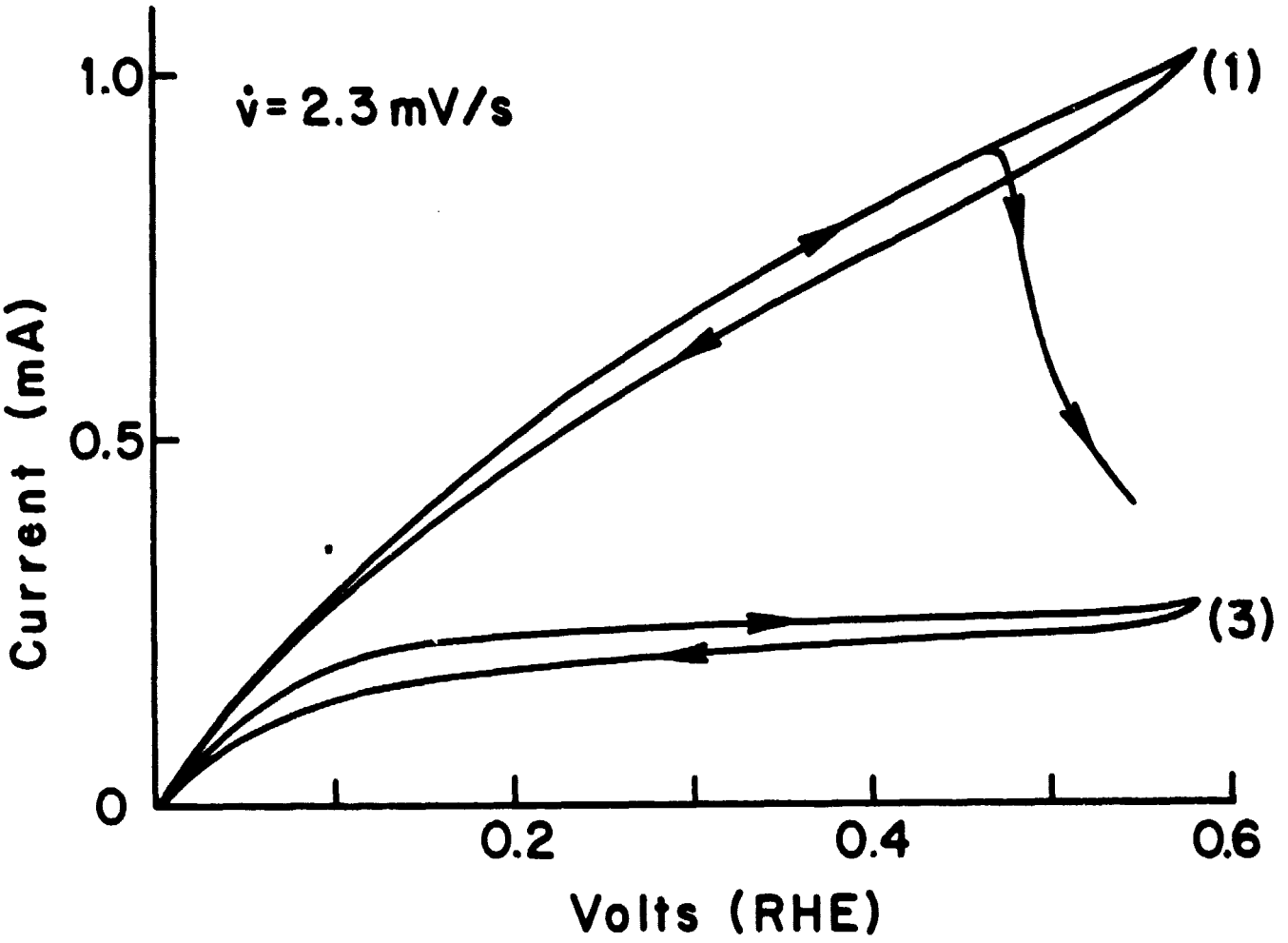

Figure 5

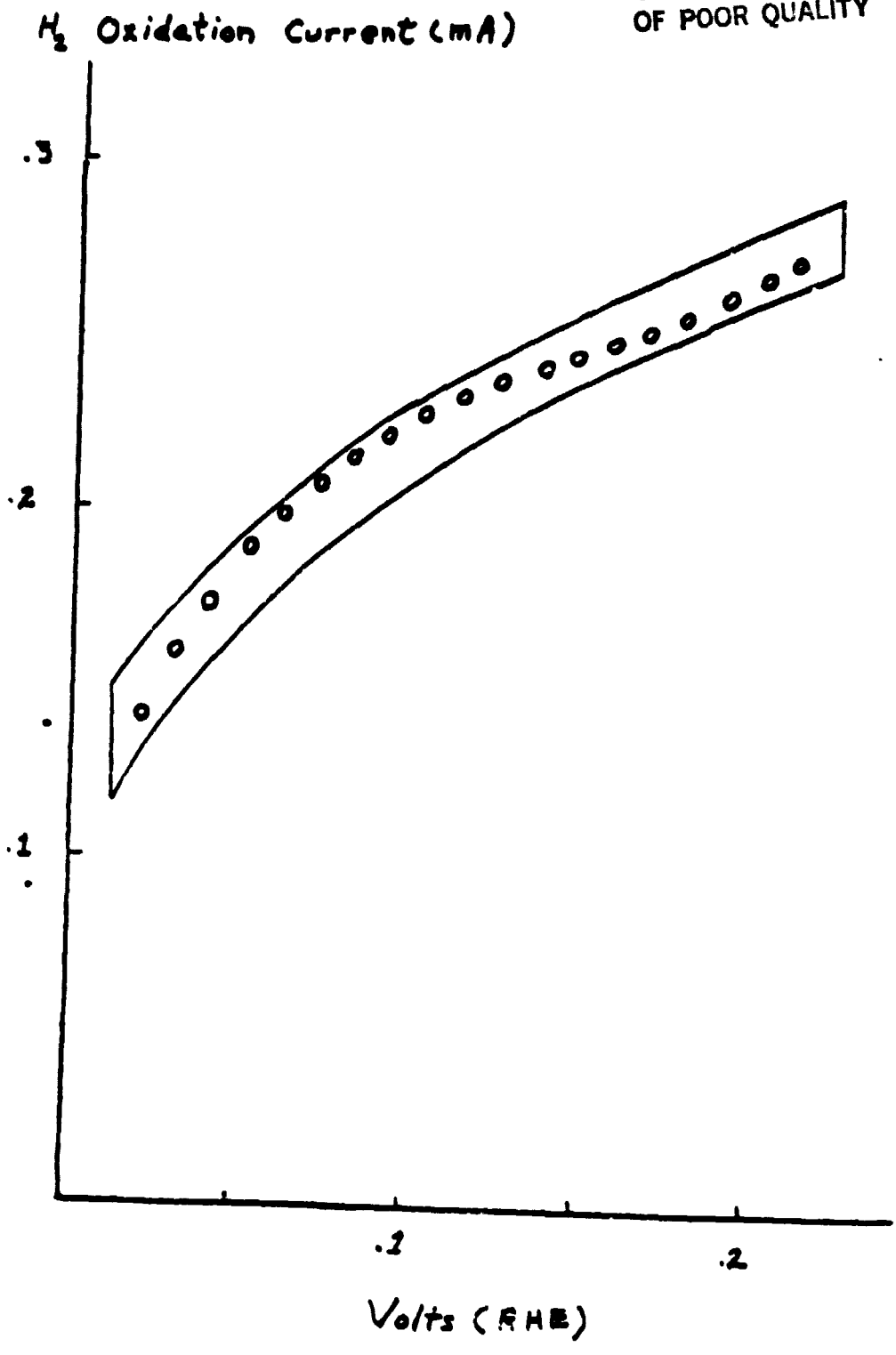

Figure 6

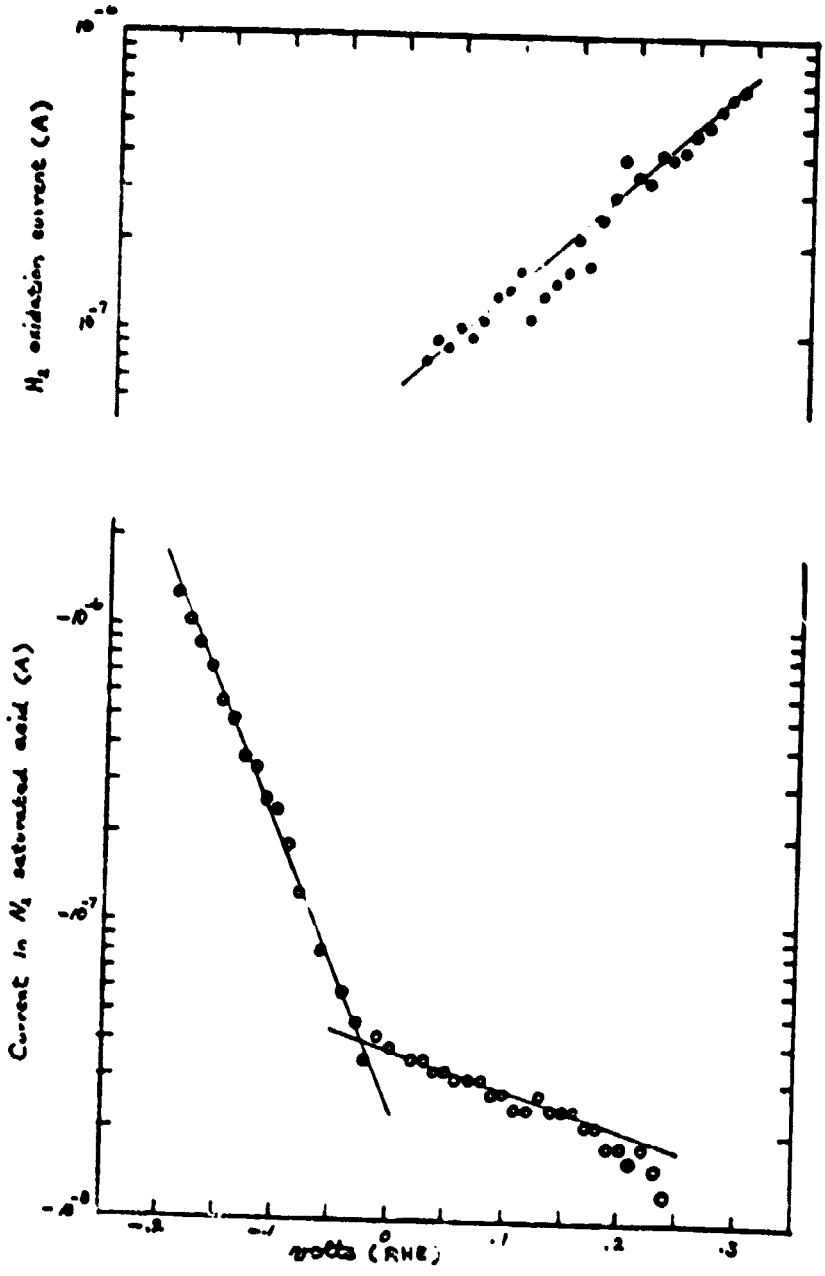

Figure 7

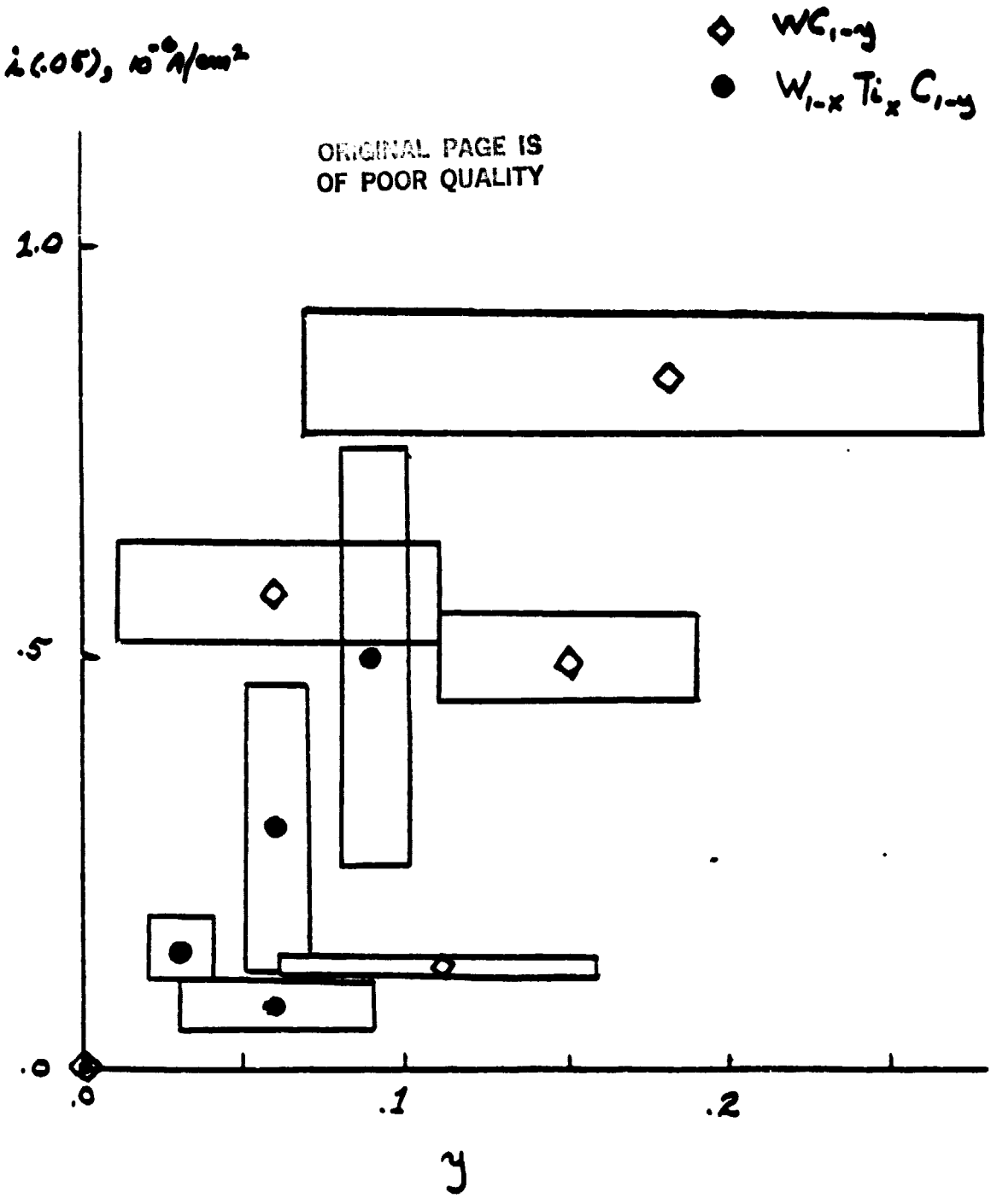

Activity at 50°C in concentrated H_3PO_4 vs C defect.

$W_{1-x}Ti_xC_{1-y}$ data weighted by $(1-x)^{-2}$

Figure 8